Can we look inside a dynamo?

Frank Stefani, Gunter Gerbeth
Forschungszentrum Rossendorf, Germany
P.O. Box 510119, D-01314 Dresden, Germany

October 6, 2000

Abstract

For a simple spherically symmetric mean-field dynamo model we investigate the possibility of determining the radial dependence of the coefficient α. Growth rates for different magnetic field modes are assumed to be known by measurement. An evolutionary strategy (ES) is used for the solution of the inverse problem. Numerically, we find quite different α-profiles giving nearly the same eigenvalues. The ES is also applied to find functions $\alpha(r)$ yielding zero growth rates for the lowest four magnetic field modes. Additionally, a slight modification of the ES is utilized for an "energetic" optimization of α^2-dynamos. The consequences of our findings for inverse dynamo theory and for the design of future dynamo experiments are discussed.

1 Introduction

At the very beginning, the question of the origin of cosmic magnetic fields was formulated as an inverse problem. "How could a rotating body such as the sun become a magnet?" was the question Larmor put in 1919 (Larmor 1919), i.e. he asked for the unknown cause of an evident effect. In the last decades, dynamo theory saw an enormous progress. Testing a large number of kinematic models in the sense of a forward problem, the inverse character of the original problem was partly pushed into the background. It seems to be only a few percent of papers on the dynamo topic which are dealing with an inverse problem in the strict sense.

In geophysics, there is a long tradition to reconstruct the tangential components of the velocity field at the core-mantle boundary from geomagnetic secular variations (see, e.g, Bloxham (1989), and references therein). But the value of this type of inverse frozen-flux modeling was called into question recently (Love 1999). The main argument of the criticism was that the removal of the diffusion term from the induction equation changes its differential order resulting possibly in a drastic change of the nature of the solutions.

Another approach to the inverse dynamo problem was formulated by Love and Gubbins (1996). In this paper, the eigenvalue equation was complemented by some regularizing functionals in order to optimize dynamo models with respect to energetic demands and smoothness properties of the arising magnetic field. However, geomagnetic observations were taken into account only in the sense that some smoothness properties of the model magnetic field were compared with those of the observed field and not in the sense of fitting the model to the actual data.

With the advent of the first successful hydromagnetic dynamo experiments (Gailitis et al. 2000; Müller and Stieglitz 2000) quite new perspectives for inverse dynamo theory come into play. Compared to cosmic bodies, much more measurement techniques and measurable quantities can be taken into account. One additional measurable quantity is the electric potential at the boundary of the dynamo module which can provide complementary information in addition to the magnetic field on the outside. Further on, in contrast to the case of cosmic bodies it is possible to apply various magnetic fields from outside and to determine the response of the dynamo on these primary fields. Those date can be collected in the regime below the critical magnetic Reynolds number (Rm) in order to predict the dynamo behaviour at larger Rm.

In connection with this, but up to now restricted to small Rm, there are some new developments concerning the determination of the velocity field from externally measured induced magnetic fields and electric potentials when primary magnetic fields are applied (Stefani and Gerbeth 1999, 2000a, 2000b). For a static homogeneous primary field and spherical geometry it was shown (Stefani and Gerbeth 2000a) that the defining scalars of the velocity can be determined except for an ambiguity of the radial dependence of their spherical harmonics expansion coefficients. Although one can try to get a reasonable guess of the unknown radial dependence by some regularization techniques, in the strict sense this dependence remains unobservable. A generalization of this method to higher Rm would amount to a combination of an eigenvalue solver (similar to the philosophy of Love and Gubbins) with a data-fitting procedure. However this approach might look like in detail, we guess that the radial dependence will remain undetectable. Roughly speaking, two two-dimensional measured quantities (radial component of magnetic field plus electric potential) allow only to determine two two-dimensional desired quantities. Actually, this radial ambiguity was the first reason for the following investigation. At least for the small Rm regime it seems clear that the necessary third dimension to determine the radial dependence can only be the time (or frequency).

Whereas a general inverse dynamo theory is still missing, it is worth to have a sidelong glance at the quite similar inverse problem in quantum mechanics. There is a huge literature on inverse scattering theory and inverse spectral theory (for an overview, see Chadan and Sabatier (1977) and Chadan et al. (1997)), and evidently many methods from quantum mechanics (Gelfand-Levitan equation, WKB methods, operator methods, etc.) remain to be adapted and utilized in

inverse dynamo theory.

In the present paper, we will pursue a less ambitious program restricting ourselves to a pragmatic treatment of a simple inverse spectral dynamo problem. It is a simple problem as it concerns spherically symmetric α^2-dynamos in which, as a slight modification of the original model of Krause and Steenbeck (1967), the radial dependence of α is assumed to be unknown. The treatment will be pragmatic in the sense that we suppose eigenvalues of only a few magnetic field modes to be "measured" and that we will try to infer the radial dependence of α from this restricted set of information.

Basically, it is our aim to get some acquaintance with the peculiarities if one tries to get information on the radial distribution of the source of dynamo action. Reminding quantum theory might be useful in the following respect: The existence of isospectral potentials is a well established fact in quantum theory. For example, it is possible to deform *continuously* the harmonic oscillator potential in such a way that all the eigenvalues are the same as for the original quadratic potential (De Lange and Raab 1991). Therefore, we should be aware of the possibility that any inversion procedure of any set (even of an infinite number) of measured eigenvalues might lead to a variety of radial α-distributions which cannot be discriminated using only their eigenvalues. For the corresponding quantum inverse problem it is known that a potential can be uniquely determined if the spectra *for two different boundary conditions* were known. A similar behaviour should also be expected for the inverse dynamo problem, but this seems to be irrelevant for any realistic measurement strategy.

Our method might have application for cosmic dynamos as well as for laboratory dynamos. Of course, a spherically symmetric α^2-dynamo model is surely too simple to explain cosmic dynamos but the general method is easily extendable to more realistic models.

The paper is structured as follows: in the second section, the used eigenvalue solver is presented and five paradigmatic types of radial dependence of α are treated as a forward problem. In the third section, the evolutionary strategy to invert the "measured" growth rates for a number of magnetic field modes into a radial dependence of α is presented. Then, we try to reconstruct five models from section 3. Numerically, we find quite different α-profiles giving nearly the same eigenvalues. Additionally, we treat two other problems which can be, at least in principle, of interest for future dynamo experiments. At first we try to find such a function $\alpha(r)$ which yields zero growth rate for the lowest four field modes. Such a profile for α might be a candidate for a (hypothetical) dynamo experiment showing such interesting effects like mode-switching. Further on, we use our code for an "energetic" optimization of α^2-dynamos. The paper closes with some remarks on possible future developments.

2 The forward problem

Shortly speaking, our approach to solve the inverse problem will be the most simple one: to solve the forward problem many times and to seek, in some appropriate manner, for those dynamo models which give eigenvalues as close as possible to the measured ones. Therefore, the present chapter on the forward problem describes also the kernel of the inverse problem solving code which will be presented in detail in the next section.

We start with the induction equation for a mean-field dynamo model restricted to a spherically symmetric α-coefficient. For the sake of simplicity, we ignore any large-scale velocity field as well as any β-effect or any anisotropic α-coefficients. The electrical conductivity σ is assumed to be constant inside a sphere of radius R and is assumed to be zero in the outer part. Then, inside the sphere, the magnetic field has to satisfy the equations (Krause and Rädler 1980)

$$\frac{\partial \boldsymbol{B}}{\partial t} = \nabla \times (\alpha \boldsymbol{B}) + \frac{1}{\mu_0 \sigma} \Delta \boldsymbol{B} \ , \quad \nabla \cdot \boldsymbol{B} = 0 \ . \tag{1}$$

At the boundary with $r = R$, the magnetic field has to match continuously to a potential field.

In the usual manner, $\mathbf{B}$ is represented as a sum of poloidal and toroidal components,

$$\boldsymbol{B} = -\nabla \times (\boldsymbol{r} \times \nabla S) - \boldsymbol{r} \times \nabla T \tag{2}$$

with the defining scalars S and T expanded in spherical harmonics according to

$$S(r,\theta,\phi) = \sum_{l=1}^{\infty} \sum_{m=-l}^{l} R\, S_l^m(r) Y_l^m(\theta,\phi) \exp \lambda_l t \tag{3}$$

$$T(r,\theta,\phi) = \sum_{l=1}^{\infty} \sum_{m=-l}^{l} T_l^m(r) Y_l^m(\theta,\phi) \exp \lambda_l t \ . \tag{4}$$

In order to simplify the notation, throughout the rest of the paper we will measure the length in units of R, the time in units of $\mu_0 \sigma R^2$, and the coefficient α in units of $(\mu_0 \sigma R)^{-1}$.

Using (2), (3) and (4), the induction equation can be transformed into the following form (Rädler 1986):

$$\lambda_l S_l = \frac{1}{r} \frac{d^2}{dr^2}(r S_l) - \frac{l(l+1)}{r^2} S_l + \alpha(r) T_l \tag{5}$$

$$\lambda_l T_l = \frac{1}{r} \frac{d}{dr} \left(\frac{d}{dr}(r T_l) - \alpha(r) \frac{d}{dr}(r S_l) \right) - \frac{l(l+1)}{r^2} (T_l - \alpha(r) S_l) \ . \tag{6}$$

Table 1: Functions $\alpha(r)$ for ten considered models.

Model	$\alpha(r)$	Model	$\alpha(r)$
a1	C	a2	$C\ (1 - 5r^2 + 12r^3 - 7r^4)$
b1	$5/3\ C\ r^2$	b2	$7/3\ C\ r^4$
c1	$15/6\ C\ (1 - r^2)$	c2	$21/12\ C\ (1 - r^4)$
d1	$10\ C\ (r^2 - r^3)$	d2	$35/6\ C\ (r^2 - r^4)$
e1	$270/13\ C\ (4/27 - r^2 + r^3)$	e2	$140/11\ C\ (1/4 - r^2 + r^4)$

Note that there is no coupling between field modes differing in the order l of the spherical harmonics. Furthermore, we have skipped the index m for the coefficients of the defining scalars as it does not show up in the equations. Note in addition that the eigenvalues λ may be complex.

At the surface $r = 1$, the boundary conditions

$$\frac{dS_l}{dr} + (l+1)S_l = T_l = 0 \tag{7}$$

must be fulfilled.

In order to have a comparable global measure of the α-effect we introduce the following definition:

$$C = 3 \int_0^1 \alpha(r) r^2 dr\ . \tag{8}$$

Of course, other definitions, e.g. one without the r^2-term in the integral, are as well conceivable. The definition used here might be sensible for the purpose of "energetic" optimization as it reflects the volume averaged intensity of α.

To solve the coupled system of equations (5) and (6) together with the boundary condition (7) we have applied a standard shooting procedure using Newton's method. This code was validated for the case of constant α as well as for some known results with a radial variation of α (Rädler 1986).

In the following, we will present the results of the forward problem for five paradigmatic models. Table 1 shows the corresponding functions explicitely. The somewhat strange numerical factors arise due to the definition (8) The examples a, b, c, d, and e represent the following types of α-profiles: type a1 gives a constant α whereas $a2$ is only a slightly modified version with a small oscillation around the constant value. Curves of type b and c are monotonically increasing and decreasing, respectively. Curves of type d and e have one maximum and one minimum between 0 and 1, respectively.

In Fig. 1 the dependence of the growth rates λ on C for the modes with $1 \leq l \leq 6$ is shown. For the sake of simplicity, we take into account only the lowest radial wavenumber $n = 1$. Admittedly, it is not completely consistent

to include, e.g., the mode with $l = 3$ and $n = 1$ having a growth rate of $\lambda(C = 0) = -33.1$ and to skip at the same time the mode with $l = 1$ and $n = 2$ having a growth rate of $\lambda(C = 0) = -20.2$ (Krause and Rädler 1980). In principle, there is no obstacle to take into account modes with higher radial wavenumbers. The restriction to $n = 1$ might suffice for the simple toy model of inverse dynamo theory as it is considered here.

Fig. 1 gives clear evidence of a dependence of the curves for different values of l and their relations to each other on the function $\alpha(r)$. For example, a monotonic increase of α (as in b1, b2) and a maximum between 0 and 1 (d1, d2) seems to make the curves for different l "converging" to each other. On the other hand, monotonic decrease (c1, c2) or a minimum (e1, e2) seems to make the curves more parallel or even more moving away. However this might be (and we will see later that this behaviour is not universal) we only note here that there are clear differences in the relations of the eigenvalues of different field modes which will be used in an inversion scheme to determine $\alpha(r)$. Apart from example a2, we used only curves with at most one maximum or minimum. In the next section we will face the problem that some oscillations (with at least one maximum and one minimum) around the treated paradigmatic model give eigenvalues which are (at least) very close to the original one.

Note that the restriction to values $C < 6$ was not voluntary as we have found (for some of the models) regions of C were no *real* eigenvalues exist. This gives evidence for the existence of oscillatory dynamos. This possibility has been discussed in a number of papers (Rädler 1986, Rädler and Bräuer 1987) and is of some interest in its own right. Only for the sake of numerical simplicity we skip this problem here. There are no principle obstacles to make the eigenvalue code fit for complex computations, too. As for the inverse problem, which will be treated in the next section, we only remark that in case that some intermediate trial function of $\alpha(r)$ are found to have no real eigenvalues, these configurations are skipped and are replaced by the next trial function.

3 The inverse problem

3.1 Evolutionary Strategies

In this section, we want to present and apply an inversion scheme using "measured" growth rates for a finite number of magnetic field modes to get the radial dependence of α. From the very beginning, we will take into account the possibility that there could exist various solutions of this kind of inverse problem, i.e. various α-profiles which can be distinguished considering, e.g., their mean quadratic curvature.

For that reason, we decided to use a regularization of the inverse problem. One convenient way of regularizing an inverse problem is to add to the usual functional of the mean squared residual deviation an additional weighted func-

tional of some appropriate norm of quantities one is looking for and to search for minima of the arising total functional. Using this so-called Tikhonov regularization approach (for an overview see, e.g., Hansen 1992), one can scale through the regularization parameter. This way one usually gets Tikhonov's L-curve. At the point of highest bending (the "knee") one can find a reasonable compromise between an optimal fitting of the model data to the measured data and a minimal norm of the desired quantity.

Here, we will slightly modify this regularization method in the following way. To begin with, we restrict the space of functions to polynomials of fourth order, excluding the term proportional to r ($\alpha(r) \sim r$ would correspond to a cusp of α at the origin which seems to be not very realistic). These polynomials are parameterized by values $\tilde{\alpha}_i$ at the fitting points $r_i = 0.25, 0.5, 0.75, 1.0$ where the polynomial expansion of $\alpha(r)$ has to fit optimally the values $\tilde{\alpha}_i$. In this first fitting procedure, however, we use an additional weighted functional which keeps the mean squared curvature more or less small. For a high regularization parameter any set of (four) values at the fitting points leads to relatively smooth curves in the space of polynomial expansion coefficients. When the regularization parameter goes to zero the fitting curve tends exactly to the parameterizing values at the fitting points. Thus, we are able to regularize the curves even before they are put into the kernel of the inversion scheme.

To put this procedure in formulae, let us assume that we have a trial set of values $\tilde{\alpha}_i$ at the fitting points $r_1 = 0.25$, $r_2 = 0.5$, $r_3 = 0.75$, and $r_4 = 1.0$. Fitting a function $\alpha(r) = a + br^2 + cr^3 + dr^4$ will be done by minimizing the functional

$$F = \sum_{i=1}^{4} (\alpha(r_i) - \tilde{\alpha}_i)^2 + p \int_0^1 (2b + 6cr + 12dr^2)^2 dr \tag{9}$$

where p denotes the regularization parameter.

After having explained the chosen parameterization, we will describe in the following the chosen minimum search procedure. We decided to use an evolutionary strategy (ES) for that purpose (for an overview see, e.g., Schöneburg, Heinzmann and Feddersen 1994). An ES is known to be an appropriate method in case of existence of several local minima. It is capable to leave local minima in order to find the global minimum of a given problem. We will sketch the philosophy of the used ES only shortly. For our particular code, we took over the scheme described by Küchler, Lehnert and Tschornack (1995).

An ES tries to utilize the principle of biological evolution for the numerical solution of (non-linear) optimization problems. Let us start with an "population" of 30 "individuals" which are vectors of parameterizing values at the fitting points. To each of those individuals a quality function Q is ascribed. In order to compute this quality function Q, we have to solve, for every considered l, the eigenvalue equation for the trial function $\alpha(r)$ which results from the vectors of parameterizing values the way described above. Having computed

the eigenvalues for the given individual we compare these eigenvalues with the measured ones and define the quality function as the mean squared residual deviation. Here, we assume the a-priori errors for all l-mode measurements to be equal. Of course, this might be corrected in any practical application.

The population evolves in the following manner: In every new generation only one child is created by one of three different kinds of reproduction which are mutation, cross-breeding, and crossing-over. For every generation the actual reproduction kind is used by random. For the relative frequency of mutation, cross-breeding, and crossing-over we have chosen the values 0.3, 0.3, and 0.4, respectively.

Mutation means that we select one "parent" by random and create from this a "child" by mutation of the parameters, i.e.

$$\tilde{\alpha}_i^C = \tilde{\alpha}_i^P + \Delta_i \gamma s \; . \tag{10}$$

Here $\tilde{\alpha}_i^C$ is the i'th parameter of the child, $\tilde{\alpha}_i^P$ is the i'th parameter of the parent, Δ_i is the spread of the corresponding parameter, γ is a mutation width and s is a normal distributed random number. It should be noted that Δ_i is large at the beginning of the evolution when a large area of the parameter space is to be covered, but that it decreases when the whole population is running into the global minimum.

Cross-breeding means that the parameters of two parents $P1$ and $P2$ which are selected by random are averaged in the child:

$$\tilde{\alpha}_i^C = 0.5 \; (\tilde{\alpha}_i^{P1} + \tilde{\alpha}_i^{P2}) \quad . \tag{11}$$

Two parents are also selected in the crossing-over, but their parameters will be mixed in the sense that for each parameter $\tilde{\alpha}_i^C$ it will be selected by random whether it comes from parent $P1$ and $P2$.

After having created a child, it must be evaluated. At first, it has to be checked whether the parameters of the child still fulfill some reasonable given constraints. If this is not the case, a new child has to be created. In the positive case, however, it is checked whether the quality function of the child fulfills the condition

$$Q_c < Q_{worst} + 0.4 \; (Q_{worst} - Q_{best}) \tag{12}$$

where Q_{worst} and Q_{best} are the quality functions of the worst and the best individual of the population, respectively. The value 0.4 is to some extend arbitrary. Evidently this factor is responsible for the fact that the ES is able to leave local minima. The chosen factor 0.4 is relatively high. The effect is a certain slow-down of the convergence but a higher reliability to find the global minimum and not to be locked in a local one. If the condition (13) is fulfilled, after cross-breeding and crossing-over the qualitatively worse parent is replaced by the child. In case of mutation, the parent is replaced, except when the parent

is the best individual of the population and the quality of the child is not better than the quality of the parent. In this special case, the worst individual of the population is replaced by the child.

Evidently, the number of individuals in every generation stays the same. The evolution can be stopped when all individuals of the population have gathered in one (hopefully: the global) minimum, e.g., when the spread of all parameters has become very small. Of course, if several minima of the quality function with nearly the same depth exist, the evolution might be locked in quite different of them, depending on the random numbers used in the evolution. In order to control this erratic behaviour, we have used the regularization scheme described above. Thus, scaling the regularization parameter p from larger to smaller values, we expect the smoothest solution to show up first and solutions with higher curvature to appear only for smaller values of p. Than, however, the mentioned erratic behaviour might be observed.

3.2 Results for the paradigmatic examples

Fig. 2 shows the results of the used ES inversion scheme for the examples a1, b1, c1, d1, and e1 from section 2. Every plot on the right hand side shows nine curves $\alpha(r)$, the first representing the exact input function which was used in the forward task for the determination of the growth rates for different l-modes. The remaining eight curves give the output of the ES inversion scheme, differing in the value of the used regularization parameter p in equation (9). As input for the inverse task, we have used the growth rates for the first 6 l-modes at $C = 4$. Reminding that we parameterize the desired functions $\alpha(r)$ by means of 4 values, 6 growth rates give evidently some redundant information.

The plots on the right hand side of Fig. 2 are similar to what is called in regularization theory "Tichonov's L-curve". On the abscissa the logarithm of the squared curvature of the output curves is given. The ordinate axis shows the logarithm of the rms of the residual deviation (i.e., the difference of the "measured" growth rates and the growth rates resulting from the output curves). For further explanation, let us consider example b1 having a quadratic $\alpha(r)$-dependence as original function (example a1 is atypical, as the original curve has curvature zero). To begin with, consider in b1 the curves for $p = 10$ and $p = 1$. Evidently, the resulting functions $\alpha(r)$ are close to a constant, e.g., the large regularization parameter p allows only for output curves of very small mean curvature. On the right hand side we see that the corresponding residual deviation for those curves are very large. Then, with decreasing p, we get three curves which are fitting reasonably to the original one. The corresponding residual deviations are decreasing drastically. But for the last three values of p ($p = 10^{-4}$, $p = 10^{-5}$, and $p = 0$) the resulting functions $\alpha(r)$ acquire some oscillatory behaviour. Looking at the right hand side plot, we see that the residual deviations for these functions are a bit higher compared to the minimum, but evidently the ES is not able to find the global minimum. A

quite similar behaviour is found for all other examples (note that for example a1 "Tikhonov's L-curve" starts already at high values of p with a small residual error, as the original curve has no curvature).

One might argue that another minimum search code would be better suited to find the absolute minimum. Note, however, that every real measurement is biased by measurement errors. Considering the value of the rms of the residual deviations on the right hand side, it seems clear that a realistic discrimination between the curves is hardly possible. Note, in addition, that our special parameterization (with a power series expansion up to fourth order) might prevent curves for smaller regularization parameter from fitting to "measured" growth rates more exactly.

Connected with this problem one could also argue that the incorporation of more measured growth rates could improve the quality of the inversion. For this purpose, we carried out a numerical test taking into account different total numbers (denoted by $NGRO$) of "measured" growth rates. For example a1 we have tested all possibilities with $4 \leq NGRO \leq 12$ at $p = 0$. Fig. 3a shows the resulting functions. Figs. 3b, 3c, and 3d give the corresponding growth rates for the exact function and all functions resulting from the inversion (Fig. 3b shows the values for all modes with $1 \leq l \leq 12$, Fig. 3c shows the details for the first modes with $1 \leq l \leq 3$, Fig. 3d shows the details for the modes with $10 \leq l \leq 12$). The result is astonishing: all the quite different functions $\alpha(r)$ shown in Fig. 3a give nearly the same growth rates for the first modes with $1 \leq l \leq 12$, apart from very small differences. Of course, our numerical method and the used parameterization with a very limited number of parameters does not allow to construct exactly those different functions $\alpha(r)$ which might give exactly the same eigenvalues. At this point we would like to suggest analytical investigations in order to identify these isospectral functions $\alpha(r)$.

For any practical application where the accuracy of the measured values will be limited the consequences are clear: there are quite different functions $\alpha(r)$ giving nearly the same growth rates. Thus, a unique determination of the radial dependence of α from the eigenvalues of different l-modes seems to be impossible. However, using some kind of regularization, we can find those α-functions giving the measured eigenvalues with minimal penalty function, e.g, with minimal quadratic curvature. Hence, it is possible to reconstruct at least α-functions of the paradigmatic types as described in section 2.

3.3 Search for α-profiles yielding level-crossing

In the following the described ES will be used to treat another problem. Whereas in the last subsection we had used growth rates resulting from known functions $\alpha(r)$ we will now search for a-priori unknown functions. Let us assume that we would know that a cosmic body has a steady magnetic field with some field modes, say, for $1 \leq l \leq 4$. If we would know (what is, of course, not very realistic) that the dynamo mechanism were only due to a spherically symmetric

Table 2: Functions $\alpha(r)$ resulting for different regularization parameter p from the ES inversion procedure for the case that the modes with $1 \leq l \leq 4$ are demanded to have zero growth rates, and their computed growth rates.

p	$\alpha(r)$	λ_1	λ_2	λ_3	λ_4
10^1	$6.84 + 0.26\,r^2 - 0.003\,r^3 - 0.045\,r^4$	8.89	5.75	-0.22	-8.89
10^0	$5.70 + 2.84\,r^2 + 0.27\,r^3 - 0.62\,r^4$	7.52	5.30	0.19	-7.61
10^{-1}	$-1.00 + 14.37\,r^2 + 4.15\,r^3 - 4.36\,r^4$	1.58	3.16	1.29	-3.29
10^{-2}	$-1.81 - 6.02; r^2 + 41.52\,r^3 - 17.43\,r^4$	-1.28	1.88	1.34	-1.89
10^{-3}	$5.42 - 73.11\,r^2 + 127.04\,r^3 - 39.13\,r^4$	-1.22	1.04	1.11	-1.18
10^{-4}	$13.89 - 168.92\,r^2 + 270.60\,r^3 - 91.85\,r^4$	0.03	-0.32	0.65	-0.32
10^{-5}	$16.73 - 269.31\,r^2 + 509.56\,r^3 - 237.76\,r^4$	-0.03	-0.31	0.80	-0.37
0	$10.92 - 99.61\,r^2 + 126.44\,r^3 - 13.17\,r^4$	0.16	0.38	0.90	-0.46

α we could ask for its radial dependence providing exactly these four marginal modes. This is a typical example our inversion scheme can be applied for.

Table 2 gives the functions resulting from the inversion, again for a number of decreasing regularization parameters p, together with the corresponding values for the first four growth rates. We actually give here the resulting power expansions in order to allow the reader to validate the results by means of a standard forward solver for spherically symmetric $\alpha(r)$.

These functions are depicted also in Fig. 4a. The dependence of the residual deviation on the curvature is again shown in Fig. 4b. Whereas for large p the growth rates differ significantly from zero, the values for smaller p are getting very close to zero. For the best fitting $\alpha(r)$ (at $p = 10^{-4}$) we have shown in Fig. 4c the dependence of the growth rates on C for $1 \leq l \leq 6$. We see clearly the level-crossing at $C \approx 8.5$.

There might also be some relevance of the considered example for laboratory dynamos. Let us assume that we were able to build a spherical dynamo and that the dynamo action of its flow were due to a spherically symmetric α. Then, a radial dependence of α corresponding to the given curves might lead to a very interesting behaviour when the back-reaction is taken into account. For example it might happen that the back-reaction changes the function $\alpha(r)$ in such a way that mode switching between the different l-modes occurs. We would like to suggest further investigation of such a model.

3.4 Optimization

Let us turn to a second problem which might also be important for laboratory dynamos. It concerns a kind of energetic optimization of the dynamo. Of course, the optimization criterion for a mean field dynamo is not as obvious as for large

Table 3: "Energetically" optimized functions $\alpha(r)$ resulting from the inversion demanding the mode $l = 1$ to have zero growth rate. C' and C'' are defined in the text.

p	$\alpha(r)$	C'	C"
10^{-1}	$6.08 - 7.93\,r^2 + 3.19\,r^3 - 0.15\,r^4$	3.10	2.96
10^{-2}	$8.36 - 28.24\,r^2 + 28.04\,r^3 - 8.89\,r^4$	2.57	1.81
10^{-3}	$11.78 - 87.25\,r^2 + 124.28\,r^3 - 48.38\,r^4$	2.06	0.96
10^{-4}	$14.24 - 154.76\,r^2 + 265.25\,r^3 - 124.58\,r^4$	1.88	0.86
10^{-5}	$14.63 - 169.03\,r^2 + 298.69\,r^3 - 144.28\,r^4$	1.87	0.91
0	$14.60 - 168.41\,r^2 + 298.35\,r^3 - 144.54\,r^4$	1.88	0.92

scale velocities. We have chosen to minimize the following functional:

$$C' = \left(3\int_0^1 \alpha^2(r) r^2 dr\right)^{1/2} \tag{13}$$

under the constraint that the mode with $l = 1$ becomes marginal. Of course, the definition (13) is to some extend arbitrary. For comparison it is also interesting to consider the quantity

$$C'' = 3\int_0^1 |\alpha(r)| r^2 dr \tag{14}$$

where we used the modulus of α instead of α itself in order not to get very small values of C'' only due to some cancellation effects along the r-axis.

To solve this problem, the described ES code had to be modified only slightly. The resulting functions, together with the corresponding values C' and C'' are given in Table 3.

We do not claim to have found the function $\alpha(r)$ with the smallest value of C' or C''. Remind that we have restricted the allowed functions to be a polynomial expansion up to fourth order. There might be quite different functions providing even lower values of C' and/or C''.

Despite some arbitrariness of the definitions of C' and C'', it is interesting to note that something like the volume averaged "amount" of α can be decreased significantly compared to the well known critical value 4.49 for the Krause-Steenbeck dynamo model.

4 Conclusions

In this paper we have tried to reconstruct the radial distribution of α from growth rates of a few l-modes of the magnetic field.

It was shown that some paradigmatic functions $\alpha(r)$ can indeed be recovered by the used evolutionary strategy if a careful regularization of the trial functions is used. With decreasing smoothing effect of the regularization, the ES erratically jumps into various local minima and the resulting functions $\alpha(r)$ can differ drastically from the original one.

Although by our simple numerical means we are not able to test the isospectrality of different α-profiles in a strict sense, the obvious existence of different minima with nearly the same quality functions seems to be more than an accident. A more precise identification of such isospectral α-profiles is highly desirable and we would like to suggest further analytical and numerical investigation in this direction.

On the other side, for any practical application (e.g. with measurement errors and only a finite number of l-modes) it is quite clear that the function $\alpha(r)$ can be determined only roughly.

A unique determination of $\alpha(r)$ would probably require knowledge of the spectra for two different boundary conditions which is, even for laboratory dynamos, not very realistic.

An obvious future task is to generalize the presented method to the oscillatory case, possibly in connection with varying conductivity (for possible astrophysical applications of this case, see Schubert and Zhang 2000). In principle, the developed ES code can be combined with any forward solver for more complicated dynamo models in order to apply the method to real cosmic or laboratory dynamos. For other than spherical geometry it might also be useful to combine the method with an forward solver based on the integral equation approach (Stefani, Gerbeth, and Rädler 2000).

References

[1] Bloxham, J.: 1989, Geophys. J. Int. **99**, 173-82

[2] Chadan, K, Sabatier, P. C: 1977, Inverse Problems in Quantum Scattering Theory, Springer, New York, Heidelberg, Berlin

[3] Chadan, K., Colton, D., Päivärinta, Rundell, W.: 1997, An Introduction to Inverse Scattering and Inverse Spectral Problems, SIAM, Philadelphia

[4] De Lange, O. L., Raab, R. E.: 1991, Operator methods in quantum mechanics, Clarendon Press, Oxford

[5] Gailitis, A., Lielausis, O., Dement'ev, S. et al.: 2000, Phys. Rev. Lett. **84**, 4365-4368

[6] Hansen, P. C.: 1992, SIAM Review **34**, 561-580

[7] Krause, F., Rädler, K.-H.: 1980, Mean-field magnetohydrodynamics and dynamo theory, Akademie-Verlag, Berlin

[8] Krause, F., Steenbeck, M.: 1967, Z. Naturforsch., **22A**, 671-675

[9] Küchler, D., Lehnert, U., Zschornack, G.: 1995, Nucl. Instr. and Meth. in Phys. Res. B **103**, 243-248

[10] Larmor, J.: 1919, Rep. Brit. Asssoc. Adv. Sci., 159-160

[11] Love, J. J., Gubbins, D.: 1996, Geophys. J. Int., **124**, 787-800

[12] Love, J. J.: 1999, Geophys. J. Int., **138**, 353-365

[13] Müller, U., Stieglitz, R.: 2000, in: F. Plunian (ed.): Proc. of the Int. Conf. "Magnetohydrodynamics at the Dawn of Third Millenium", Giens, France, September 17-22, 2000, Grenoble 2000, 175-182

[14] Rädler, K.-H.: 1986, unpublished manuscript

[15] Rädler, K.-H., Bräuer, H.-J.: 1987, Astron. Nachr. **308**, 127-131

[16] Schubert, G., Zhang, K.: 2000, http://arXiv.org/abs/astro-ph/0002529

[17] Schöneburg, F., Heinzmann, F., Feddersen, S.: Genetische Algorithmen und Evolutionsstrategien, Addison-Wesley, Reading, Mass.

[18] Stefani, F., Gerbeth, G.: 1999a, Inverse Problems **15**, 771-786

[19] Stefani, F., Gerbeth, G.: 2000a, Inverse Problems **16**, 1-9

[20] Stefani, F., Gerbeth, G.: 2000b, Meas. Sci. Technol. **11**, 758-765

[21] Stefani, F., Gerbeth, G., Rädler, K.-H.: 2000, Astron. Nachr. **321** 65-73

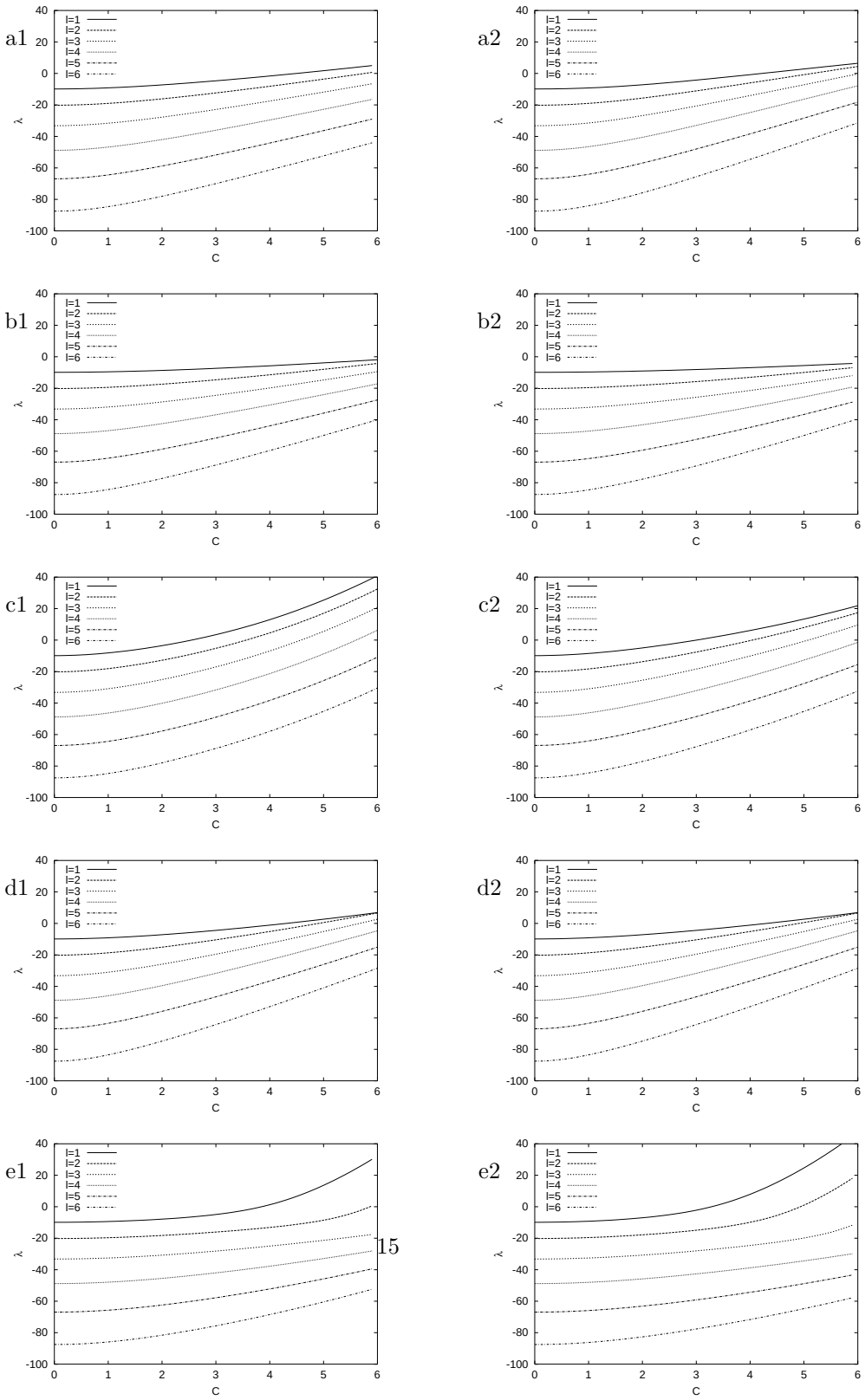

Figure 1: Growth rates for $1 \leq l \leq 6$ for the models given in table 1.

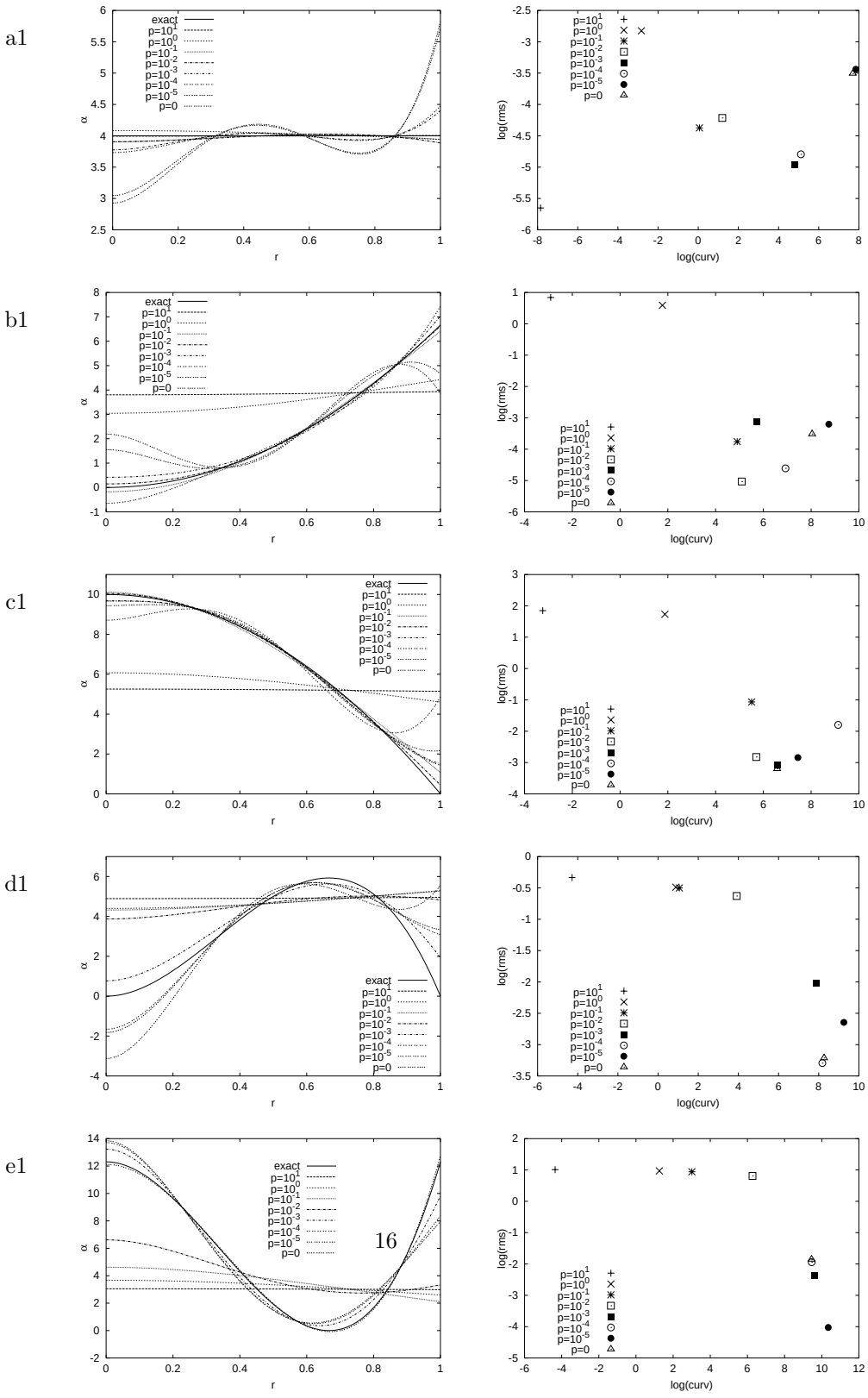

Figure 2: Left column: original functions $\alpha(r)$ and functions resulting from the ES inversion procedure for different regularization parameters p. Right column: dependence of the rms of the residual error on the mean squared curvature of the resulting function. The cases a1, b1, c1, d1, and e1 correspond to the models considered in section 2.

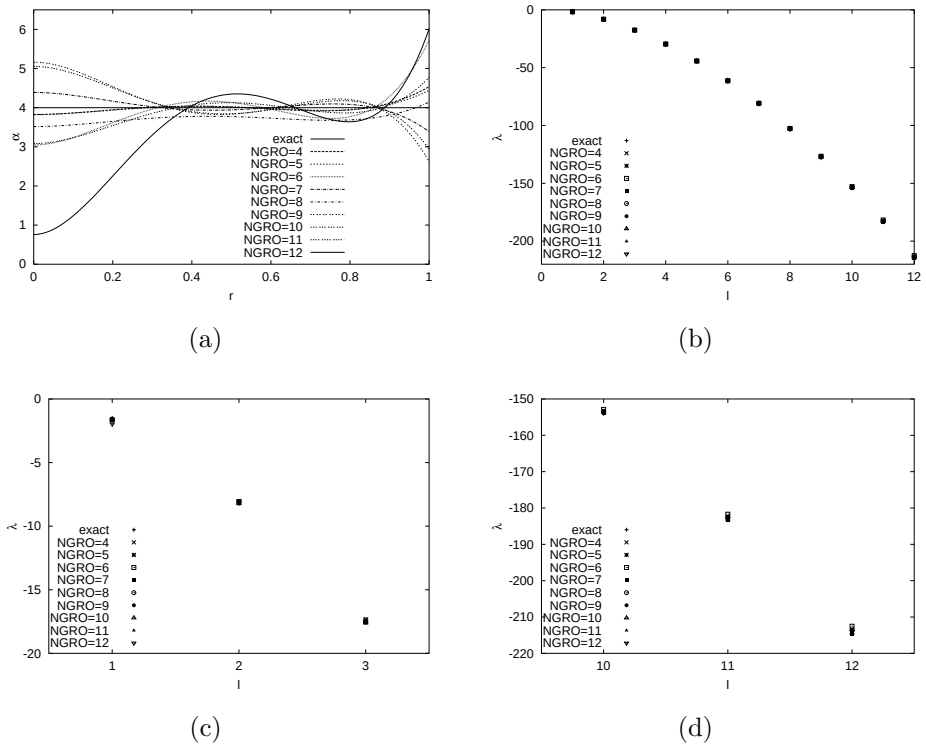

Figure 3: Results of the ES inversion scheme for model a1 using different numbers $NGRO$ of "measured" growth rates for modes with $1 \leq l \leq NGRO$. The functions are shown in (a). In (b) the growth rates (for $1 \leq l \leq 12$ of all resulting curves are plotted. The same in (c) and (d), but detailed for the lowest three l and the highest three l. Evidently, the resulting growth rates for quite different functions $\alpha(r)$ are practically indistinguishable.

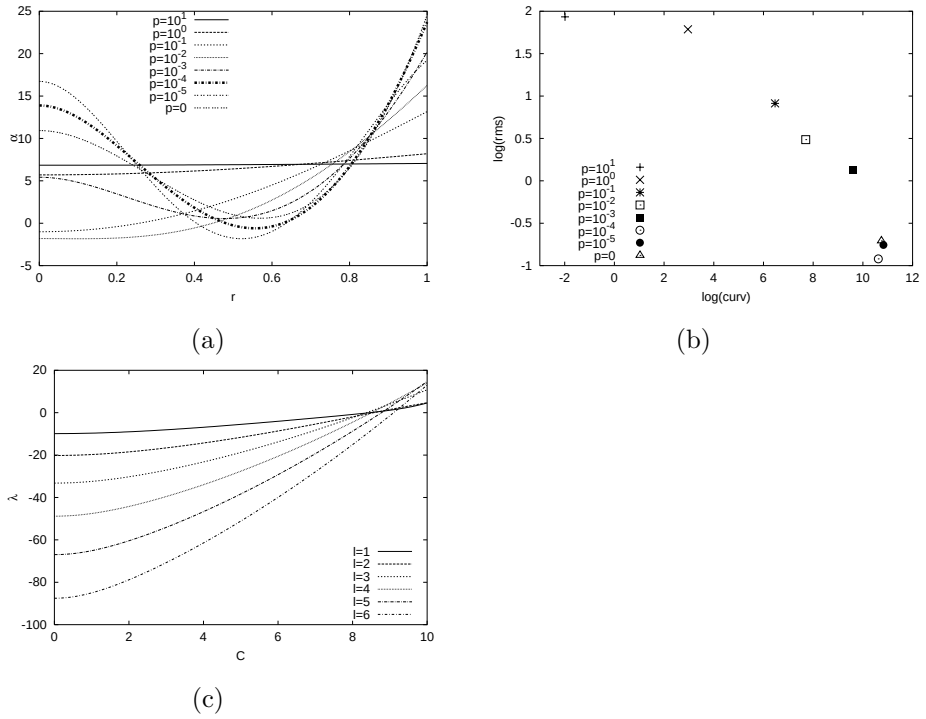

Figure 4: Functions $\alpha(r)$ resulting for different regularization parameter p from the ES inversion procedure for the case that the modes with $1 \leq l \leq 4$ are demanded to have zero growth rates (a), the corresponding dependence of the residual error on the curvature (b). For the special regularization parameter $p = 10^{-4}$, the solution of the forward problem for the first 6 l-modes is depicted in (c). The "level-crossing" at $C \approx 8.5$ is evident.

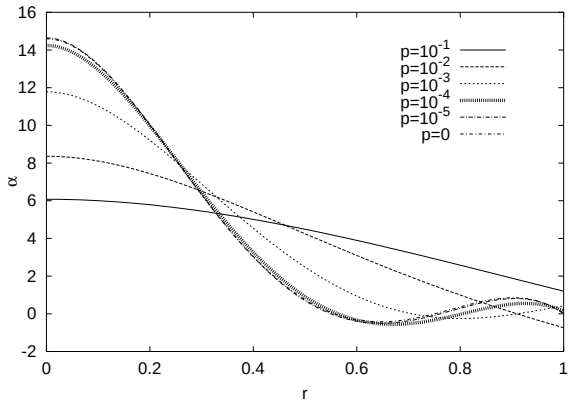

Figure 5: "Energetically" optimized functions $\alpha(r)$ resulting from the inversion demanding the mode with $l = 1$ to have zero growth rate.